Gazi Med J 2026;37(2):157-165

DOI: http://dx.doi.org/10.12996/gmj.2025.4598

Polyethylenimine-Mediated Delivery of miR-379-5p Suppresses MTDH and FOXP2 in Colorectal Cancer Cells

Polietilenimin Aracılı miR-379-5p Taşınmasının, Kolorektal Kanser Hücrelerinde MTDH ve FOXP2'yi Baskılaması

Ekin Çelik[1], Ertan Kanbur[2], Cem Bayram[3], Çağrı Aydoğan[4], Miraç Berkay Köksal[4], Selahattin Ata Aydın[4], Yiğit Emre Kurt[4]

[1]Department of Medical Biology, Kırşehir Ahi Evran University, Faculty of Medicine, Kırşehir, Türkiye
[2]Department of Immunology, Kırşehir Ahi Evran University, Faculty of Medicine, Kırşehir, Türkiye
[3]Department of Nanotechnology and Nanomedicine, Hacettepe University, Graduate School of Science and Engineering, Ankara, Türkiye
[4]Kırşehir Ahi Evran University, Faculty of Medicine, Kırşehir, Türkiye

ABSTRACT

Objective: To develop an optimized polyethylenimine (PEI)-based nanocarrier for the intracellular delivery of miR-379-5p and to evaluate its efficacy in suppressing the oncogenic targets metadherin (MTDH) and Forkhead box P2 (FOXP2) in KRAS-wild-type colorectal cancer cells.

Methods: PEI-miRNA nanocomplexes were synthesized at various nitrogen-to-phosphate (N:P) ratios and characterized via dynamic light scattering, zeta potential measurements, and scanning electron microscopy (SEM). Cytotoxicity was assessed in Caco-2 cells using MTT assays to determine the optimal therapeutic concentration. Gene silencing efficiency and intracellular uptake were quantified using reverse transcription quantitative polymerase chain reaction.

Results: The formulation prepared at an N:P ratio of 20:1 exhibited optimal physicochemical properties, featuring a mean hydrodynamic diameter of ~254 nm, a compact spherical morphology, and a highly positive zeta potential (+56.9 mV). At the optimized concentration of 50 nM, the nanocomplexes maintained favorable cell viability while facilitating significant intracellular accumulation of miR-379-5p. Consequently, this delivery strategy achieved robust downregulation of MTDH and FOXP2 expression compared to naked miRNA treatment.

Conclusion: The optimized PEI-miRNA nanocomplexes effectively overcome delivery barriers, enabling successful gene silencing in Caco-2 cells. By restoring the miR-379-5p regulatory axis and suppressing

ÖZ

Amaç: Hücre içi miR-379-5p taşınması için optimize edilmiş polietilenimin (PEI) temelli bir nanotaşıyıcı geliştirilmesi ve bu sistemin, KRAS-wild tip kolorektal kanser hücrelerinde onkojenik hedefler olan metadherin (MTDH) ve Forkhead box P2 (FOXP2) üzerindeki baskılayıcı etkinliğinin değerlendirilmesi amaçlanmıştır.

Yöntemler: PEI-miRNA nanokompleksleri, farklı azot/fosfat (N:P) oranlarında sentezlenmiş ve dinamik ışık saçılımı, zeta potansiyel ölçümleri ile taramalı elektron mikroskobu (SEM) kullanılarak karakterize edilmiştir. Sitotoksisite, optimal terapötik konsantrasyonu belirlemek amacıyla Caco-2 hücrelerinde MTT testi ile değerlendirilmiştir. Gen susturma etkinliği ve hücre içi alım, gerçek zamanlı ters transkripsiyon kantitatif polimeraz zincir reaksiyonu ile nicel olarak analiz edilmiştir.

Bulgular: N:P oranı 20:1 olan formülasyon, yaklaşık 254 nm ortalama hidrodinamik çap, kompakt küresel morfoloji ve yüksek pozitif zeta potansiyeli (+56,9 mV) ile en uygun fizikokimyasal özellikleri göstermiştir. Optimize edilen 50 nM konsantrasyonda, nanokompleksler uygun hücre canlılığını korurken miR-379-5p'nin hücre içinde anlamlı düzeyde birikimini sağlamıştır. Buna bağlı olarak, bu taşıma stratejisi çıplak miRNA uygulamasına kıyasla MTDH ve FOXP2 ekspresyonunda güçlü bir azalma sağlamıştır.

Sonuç: Optimize edilmiş PEI-miRNA nanokompleksleri, taşınma engellerini etkili biçimde aşarak Caco-2 hücrelerinde başarılı gen

Cite this article as: Çelik E, Kanbur E, Bayram C, Aydoğan Ç, Köksal MB, Aydın SA, et al. Polyethylenimine-mediated delivery of miR-379-5p suppresses MTDH and FOXP2 in colorectal cancer cells. Gazi Med J. 2026;37(2):157-165

Address for Correspondence/Yazışma Adresi: Ekin Çelik, Department of Medical Biology, Kırşehir Ahi Evran University, Faculty of Medicine, Kırşehir, Türkiye
E-mail / E-posta: ekin.celik@ahievran.edu.tr
ORCID ID: orcid.org/0000-0003-1966-3907

Received/Geliş Tarihi: 04.12.2025
Accepted/Kabul Tarihi: 20.12.2025
Publication Date/Yayınlanma Tarihi: 31.03.2026

ABSTRACT

FOXP2, this system constitutes a promising molecular platform for targeted RNAi-based interventions in colorectal malignancy.

Keywords: Colorectal cancer, polyethylenimine, miR-379-5p, gene delivery, nanoparticles, RNA interference

ÖZ

susturulmasını mümkün kılmıştır. miR-379-5p düzenleyici ekseninin yeniden kurulması ve FOXP2'nin baskılanması yoluyla bu sistem, kolorektal malignitelerde hedefe yönelik RNA girişimi (RNAi) temelli uygulamalar için umut verici bir moleküler platform oluşturmaktadır.

Anahtar Sözcükler: Kolorektal kanser, polietilenimin, miR-379-5p, gen taşınımı, nanopartiküller, RNA girişimi

INTRODUCTION

Colorectal cancer (CRC) is one of the most prevalent malignancies and remains a leading cause of cancer-related mortality worldwide, representing a persistent global health challenge due to its high morbidity and mortality rates (1). Conventional treatment approaches such as surgery, chemotherapy, and radiotherapy are frequently applied in clinical practice. However, their therapeutic efficacy is markedly reduced in advanced or metastatic stages of the disease. These limitations are exacerbated by the severe treatment-associated toxicities and the development of resistance. These factors not only diminish treatment outcomes but also significantly increase the risk of recurrence, necessitating novel therapeutic strategies (2).

Recent advances in molecular oncology have highlighted gene-based therapeutic approaches, particularly RNA interference, as promising alternatives for overcoming these challenges. RNAi represents a highly specific gene-silencing mechanism that can suppress oncogenes or other disease-driving genes, thereby inhibiting tumor initiation, progression, and metastasis (3). In the context of CRC, RNAi-based therapies are attracting increasing attention for their ability to modulate pathways involved in cell proliferation, angiogenesis, invasion, and chemoresistance, offering a powerful tool for personalized and precision-targeted interventions (4-6). However, the clinical translation of RNAi therapeutics is severely hindered by physiological delivery barriers. Naked RNA molecules are inherently unstable; they are subject to rapid degradation by serum nucleases and, due to their hydrophilicity and negative charge, cannot efficiently traverse the cellular membrane (7). These limitations necessitate the development of advanced delivery platforms that can enhance the stability of RNA molecules, protect them against enzymatic degradation, and ensure efficient intracellular delivery (8-10).

Among synthetic carriers, cationic polymers, particularly polyethylenimine (PEI), have emerged as a gold standard for nucleic acid delivery in cancer research (11-14). The high density of positively charged amino groups in PEI enables strong electrostatic interactions with the negatively charged phosphate backbone of RNA, facilitating the formation of stable polyelectrolyte complexes (15,16). These complexes not only shield RNA molecules from enzymatic degradation but also potentially protect them from nonspecific binding to serum proteins, thereby prolonging circulation time and preserving biological activity. Furthermore, PEI uniquely promotes intracellular uptake via endocytosis and facilitates the "proton sponge effect," enabling endosomal escape, a critical step for functional gene silencing. Importantly, the structural diversity of PEI, which is available in both linear and branched configurations, affords considerable flexibility; branched PEI typically achieves higher transfection efficiency, whereas linear PEI is associated with reduced cytotoxicity, allowing optimization of the carrier system according to specific therapeutic requirements (17,18). These unique properties position PEI as a valuable candidate for advancing RNAi-based therapeutic strategies in colorectal cancer, where overcoming delivery challenges remains the key barrier to clinical translation (19-21).

Despite these advantages, the clinical utility of PEI is often restricted by biocompatibility issues. High-molecular-weight PEI, while efficient, is associated with pronounced cytotoxicity (22). To address these limitations, research has increasingly focused on the use of low-molecular-weight PEI derivatives or chemically modified forms to reduce toxicity while preserving or enhancing gene transfer efficiency (23,24). Accordingly, there is a pressing need for innovative delivery systems capable of safely and selectively transporting RNA molecules, particularly in malignancies with limited therapeutic options, such as colorectal cancer.

Among the therapeutic candidates for RNAi-based strategies, microRNAs have attracted considerable attention due to their ability to regulate multiple oncogenic pathways simultaneously. Specifically, miR-379-5p has been identified as a potent tumor suppressor with activity reported in several malignancies. Previous studies have demonstrated that miR-379 exerts anti-tumorigenic effects by inhibiting cell proliferation, inducing cell cycle arrest, and reducing metastatic potential (25-28). Its tumor-suppressive functions have been described in breast, ovarian, and prostate cancers; its function and therapeutic potential in colorectal cancer remain underexplored (25,29,30). One such potential target is the Forkhead box P2 (FOXP2). The role of FOXP2 in CRC is complex and context-dependent. While some studies suggest a tumor-suppressive function in KRAS-mutant contexts, recent evidence highlights that high FOXP2 expression is significantly correlated with poor overall survival in KRAS-wild-type CRC patients (31-33). Given that Caco-2 cells represent a KRAS-wild-type model, we hypothesized that FOXP2 may function as a driver of malignancy in this specific genetic background.

Consequently, this study aims to evaluate the therapeutic relevance of delivering miR-379-5p via PEI nanocomplexes for suppressing FOXP2 and metadherin (MTDH). We used these nanocomplexes to enhance intracellular uptake while minimizing cytotoxicity, thereby providing initial evidence for the efficacy of PEI-mediated delivery of this specific miRNA. Collectively, these findings offer a novel framework for the rational design of targeted RNAi-based interventions in colorectal malignancy.

MATERIALS AND METHODS

Synthesis of PEI-miRNA Nanocomplexes

Polyethylenimine (PEI; Sigma, cat. no. 408719) was selected as the carrier polymer and was complexed with microRNA-379-5p (miRNA mimic; Qiagen) at varying concentrations to obtain nanocomplexes. The complexes were subsequently characterized to determine the optimal N:P ratio.

For synthesis, miRNA solutions (0.1 mM) prepared in NaCl were incubated with PEI solutions at N:P ratios of 5:1, 10:1, 15:1, and 20:1. Incubations were performed at room temperature, with gentle mixing on a magnetic stirrer when required. The N:P ratio was calculated according to the following formula (34):

$$m_{(polymer)} = n_{(miRNA)} \times \text{number of phosphate groups} \times MW_{(protonatable\ units)} \times (N:P)$$

where m represents the required polymer mass, n represents the number of moles of miRNA, N denotes the number of nitrogen groups, and P denotes the number of phosphate groups.

Characterization of PEI-miRNA Complexes

Physicochemical Characterizations

DLS and Zeta Potential

The hydrodynamic diameter and surface charge of the nanocomplexes were determined using a Zetasizer Nano ZSP (Malvern Instruments, UK). Complexes were prepared at the optimized N:P ratio and were diluted 1:10 in nuclease-free water immediately prior to measurement. DLS measurements were performed at 25 °C with a backscattering angle of 173°. Each sample was analyzed in triplicate, and mean ± standard deviation (SD) values were recorded. Zeta potential was measured using disposable folded capillary cells, with three independent runs performed per sample.

Morphological Characterization (SEM)

The surface morphology and size distribution of the optimized PEI-miRNA nanocomplexes (N:P 20:1) were examined using a scanning electron microscope (Tescan GAIA3, USA). Prior to imaging, the nanocomplex dispersion was diluted in nuclease-free water to minimize particle aggregation. A droplet of the suspension was deposited onto a clean silicon wafer and allowed to air-dry at room temperature for 24 hours. To ensure electrical conductivity and prevent surface charging under the electron beam, the dried samples were sputter-coated with a thin layer of gold/palladium. Imaging was performed under high-vacuum conditions at an accelerating voltage of 5-10 kV.

Gel Retardation Assay

Complex formation between PEI and miRNA was assessed by agarose gel electrophoresis, as described previously (34). Nanocomplexes prepared at different N:P ratios were loaded onto 2% agarose gels and electrophoresed at constant voltage for 15 min. Gels were visualized using a ChemiDoc-It Imager (UVP, USA). A decrease in miRNA fluorescence intensity in the miRNA-PEI complex was expected, reflecting complexation with PEI and a reduction in free phosphate groups.

Biological Evaluation

The biological performance of the PEI-miRNA nanocomplexes was assessed through cytotoxicity assays, transfection studies, and gene expression analysis in colorectal cancer cells.

Cytotoxicity

Cell viability was determined using the MTT assay (211091, Abcam, UK). Caco-2 cells were seeded in 96-well plates and incubated with PEI-miRNA nanocomplexes at the selected concentrations for 48 h. Following treatment, MTT solution was added to each well, and cells were incubated to allow formazan crystal formation. Crystals were solubilized in an appropriate solvent, and the absorbance was measured spectrophotometrically at 570 nm. Each experimental and control group was analyzed in eight replicates.

Transfection

Caco-2 cells were cultured in DMEM (Life Sciences, USA) supplemented with 10% fetal bovine serum (FBS, Gibco, USA) at 37 °C in a humidified incubator with 5% CO_2. For transfection, 3×10^6 cells were seeded in 6-well plates and allowed to adhere for 12 h. The medium was then replaced with serum-free DMEM containing either naked miRNA or PEI-miRNA complexes, which were synthesized in this study, at a final concentration of 50 nM miRNA. After 4 h of incubation, the medium was replaced with DMEM containing 10% FBS, and the cells were cultured for an additional 48 h before harvest.

Gene Expression

Real-time PCR was performed to confirm miR-379-5p internalization and evaluate its effect on target gene expression. Total RNA, including miRNAs, was isolated from transfected and control cells. Separate cDNA synthesis protocols were employed for the determination of miRNA and mRNA levels; miRNA analyses were performed using stem-loop RT primers (Integrated DNA Technologies, USA), whereas mRNA analyses were conducted using a standard oligo-dT/reverse transcriptase-based kit protocol. Real-time experiments were conducted using the PowerUp SYBR Green Master Mix (Thermo Scientific, USA) on a LightCycler 480 system (Roche, Switzerland). The comparative Ct method was applied to determine relative expression levels of miR-379-5p and its target genes FOXP2 and MTDH (27,35). β-Actin (ACTB) and U6 snRNA were used as internal reference genes. Primers for U6 snRNA were purchased from ABM (Canada), and all primer sequences are listed in Table 1.

Statistical Analysis

All experiments were performed with at least three independent biological replicates. For the MTT cytotoxicity assay, each condition was tested in eight technical replicates (n = 8). For transfection and real-time PCR analyses, three independent experiments were conducted with three technical replicates per sample (n = 3). For physicochemical characterization (DLS, zeta potential), three independent preparations were analyzed (n = 3). Data were expressed as mean ± SD. Statistical analyses were performed using GraphPad Prism 9.0 (GraphPad Software, USA). Comparisons between two groups were assessed using unpaired Student's t-test, while one-way analysis of variance (ANOVA) with Tukey's post-hoc test was applied for multiple group comparisons. A p-value of <0.05 was considered statistically significant.

RESULTS

DLS and Zeta Potential

Dynamic light scattering (DLS) analysis of the PEI formulations revealed a dominant sub-micron population in all samples. Intensity-weighted main peaks ranged from ~215 to 865 nm. While a minor fraction of micron-sized aggregates (~5-5.5 µm) was detected, it represented a negligible portion of the total intensity distribution (<3% total area) and did not dominate the sample properties. Therefore, only the dominant sub-micron peaks are reported in Table 2 because they represent the functionally relevant nanoparticle population that drives cellular uptake.

Zeta potential measurements in water at 25 °C confirmed that all three NP concentrations were strongly cationic. The principal peaks ranged from approximately +10 to +56 mV, representing >90% of the particle population. Overall, the cationic polymer NPs form positively charged sub-micron dispersions; the high positive zeta potentials are consistent with efficient coating by the polymer and provide sufficient electrostatic stabilization to prevent functional aggregation under measurement conditions.

Among the tested formulations, the 20:1 PEI:NP ratio was selected for further studies based on its physicochemical profile. This formulation yielded nanoparticles with a mean hydrodynamic diameter of 254.6 ± 48.9 nm and a markedly high positive zeta potential of +56.9 ± 5.72 mV. Across the series (5:1 to 20:1), increasing the proportion of cationic polymer resulted in a gradual decrease in particle size and a concomitant increase in surface charge, indicating more efficient complexation/coating and the formation of more compact, densely charged particles. The particle size of approximately 200-300 nm remains suitable for biomedical applications, while the high positive zeta potential is expected to provide strong electrostatic stabilization and reduced aggregation. Taken together, these characteristics identify the 20:1 formulation as the most favorable candidate for subsequent biological evaluation; therefore, all following experiments were performed using this formulation.

Morphological Characterization

Scanning electron microscopy (SEM) was employed to validate the hydrodynamic size measurements and visualize the topography of the nanocomplexes. The SEM micrographs revealed that the optimized formulation (N:P 20:1) formed nanoparticles with a distinct, spherical morphology and a relatively smooth surface texture (Figure 1). The particles appeared compact, with most displaying diameters in the range of ~180 to 220 nm. Notably, the size observed via SEM was slightly smaller than the hydrodynamic diameter obtained by DLS (~254 nm). This difference is expected and can be attributed to the dehydration of the nanocomplexes during SEM sample preparation, which results in the collapse of the hydration shell and a slight shrinkage of the polymeric matrix, in contrast to the swollen state measured in the aqueous phase by DLS. Consistent with the DLS polydispersity data, occasional aggregates were also observed in the dry state.

Gel Retardation Assay

The complexation efficiency of PEI with miRNA was assessed via agarose gel electrophoresis. As expected, naked miRNA (Lane A) migrated freely through the gel matrix, appearing as a distinct band, consistent with its low molecular weight and negative charge. In contrast, at the optimized N:P ratio of 20:1 (Lane B), the miRNA was completely retained in the loading well. The complete absence of a migrating band in this lane confirms that the cationic PEI successfully neutralized the anionic phosphate backbone of the miRNA, resulting in the formation of stable, large-molecular-weight nanocomplexes with no electrophoretic mobility (Figure 2).

Cell Viability

Cell viability assays were performed to evaluate the cytotoxicity of the 20:1 PEI-miRNA nanoparticles at increasing miRNA concentrations (10, 50, and 100 nM). Treatment with 10 nM miRNA-PEI complexes did not appreciably affect cell viability compared with the untreated control, which remained close to 100%. Similarly, exposure to 50-nM complexes preserved high viability, with values remaining above ~90%.

Table 1. Primer sequences used in the study.

	F primer (5'-3')	R primer (5'-3')
miRNA-379-5p	GCGCGTGGTAGACTATGGAA	AGTGCAGGGTCCGAGGTATT
ACTB	CACCATTGGCAATGAGCGGTT	AGGTCTTTGCGGATGTCCACGT
MTDH	GGAGTCAAGACACTGGAGATG	GGGTTGATTACGGCTAACATCC
FOXP2	CAACAGCAGCAGCCAGGA	GAGGCCCCAGTCTCCCTA

FOXP2: Forkhead box P2, MTDH: Metadherin, ACTB: β-actin.

Table 2. Physicochemical characterization of the nanoparticle formulations.

Formulation	Hydrodynamic diameter (nm)	Zeta potential (mV)	PDI
5:1	789.7 ± 75.2	10.1 ± 6.99	0.706
10:1	464 ± 45.4	26.03 ± 7.60	0.444
15:1	302.2 ± 80.23	34.5 ± 11.40	0.518
20:1	254.6 ± 48.88	56.9 ± 5.72	0.386

PDI: Polydispersity index.

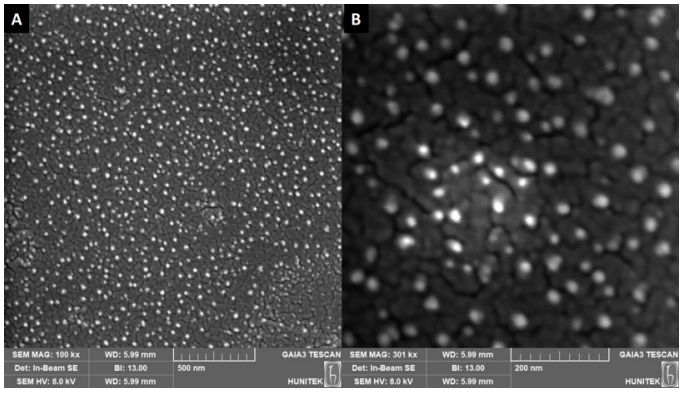

Figure 1. Morphological characterization of PEI-miRNA nanocomplexes via scanning electron microscopy (A) Representative micrograph acquired at 100 kx magnification, illustrating the general distribution and dispersion of the optimized nanocomplexes (N:P 20:1). The scale bar represents 500 nm. (B) High-magnification view (301 kx) detailing the distinct spherical morphology and compact structure of the nanoparticles. The scale bar represents 200 nm. Images are representative of three independent preparations (n = 3).

PEI: Polyethylenimine.

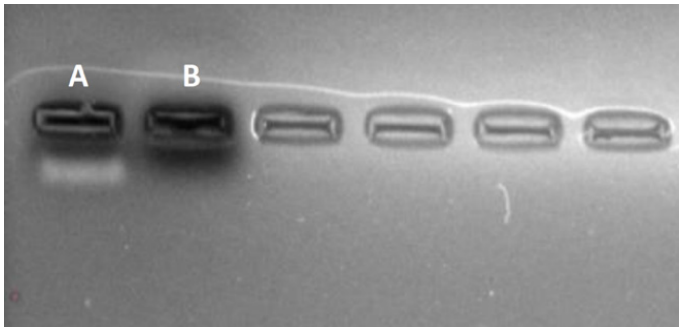

Figure 2. Assessment of miRNA complexation efficiency by agarose gel electrophoresis. The electrophoretic mobility of naked miR-379-5p and PEI-miRNA nanocomplexes was analyzed on a 2% agarose gel. (A) Naked miRNA, exhibits free migration corresponding to its negative charge (B) PEI-miRNA nanocomplexes prepared at a 20:1 ratio show complete retardation, confirming successful complexation. The image is representative of three independent experiments (n = 3).

PEI: Polyethylenimine.

In contrast, treatment with 100 nM miRNA-PEI nanoparticles resulted in a marked reduction in cell viability to approximately 65-70%. These findings indicate that the 20:1 PEI-miRNA formulation is well tolerated at lower concentrations (≤50 nM), whereas higher doses induce a clear, concentration-dependent cytotoxic effect (Figure 3). Based on these findings, 50 nM miRNA in the 20:1 PEI-miRNA formulation was selected for subsequent experiments, as it ensured efficient delivery while maintaining high cell viability.

Gene Expression

To validate the functional intracellular delivery of the cargo, the expression levels of downstream target genes MTDH and FOXP2 were quantified via reverse transcription quantitative polymerase chain reaction (RT-qPCR). As anticipated, treatment with naked miR-379-5p had a negligible impact on gene expression relative to the

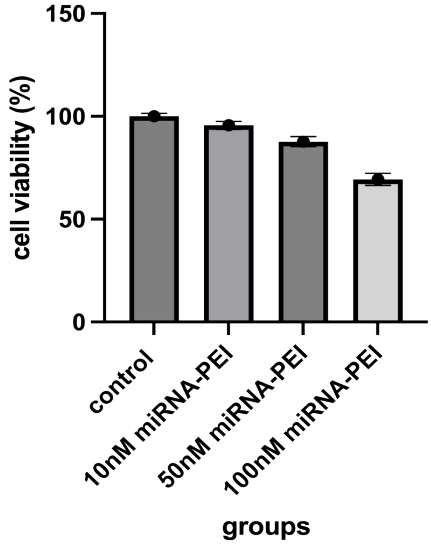

Figure 3. Cytotoxicity profile of PEI-miRNA nanocomplexes in colorectal cancer cells. Cell viability of Caco-2 cells was evaluated using the MTT assay after 48 h of incubation with PEI-miRNA nanocomplexes (N:P ratio 20:1) at miRNA concentrations of 10, 50, and 100 nM. Data are presented as the percentage of viable cells relative to the untreated control group (set to 100%). Results represent the mean ± SD of three independent experiments (n=3). Statistical significance was assessed using one-way ANOVA.

SD: Standard deviation, ANOVA: Analysis of variance, PEI: Polyethylenimine.

control, an effect attributed to the poor cellular uptake of free RNA. In contrast, the optimized PEI-miRNA nanocomplexes facilitated a significant downregulation of both targets. Specifically, MTDH mRNA levels were reduced by approximately 20% compared with the control group ($p < 0.001$); this suppression was significantly more potent than that of the naked miRNA treatment ($p < 0.01$) (Figure 4A). Similarly, FOXP2 expression exhibited a significant decrease (~16%) relative to control ($p < 0.01$), further confirming the superior transfection efficiency of the PEI-complexed formulation compared with naked miRNA ($p < 0.05$) (Figure 4B).

To verify that the observed downregulation of MTDH and FOXP2 was driven by the successful cellular internalization of the therapeutic cargo, the intracellular levels of miR-379-5p were quantified via RT-qPCR. Naked RNA molecules are known to possess poor membrane permeability due to their negative charge and hydrophilicity. Consistent with this, cells treated with naked miR-379-5p exhibited only a marginal, non-significant increase in intracellular miRNA levels compared to the untreated control (Figure 5). In contrast, the delivery of miR-379-5p via the optimized PEI nanocarrier (N:P 20:1) resulted in a statistically significant increase in intracellular miRNA abundance relative to both the control ($p < 0.01$) and the naked miRNA group ($p < 0.05$). These results confirm that the PEI nanocarrier effectively facilitates the transmembrane transport and intracellular accumulation of miR-379-5p in Caco-2 cells, validating the transfection efficiency required for functional gene silencing of the target oncogenes.

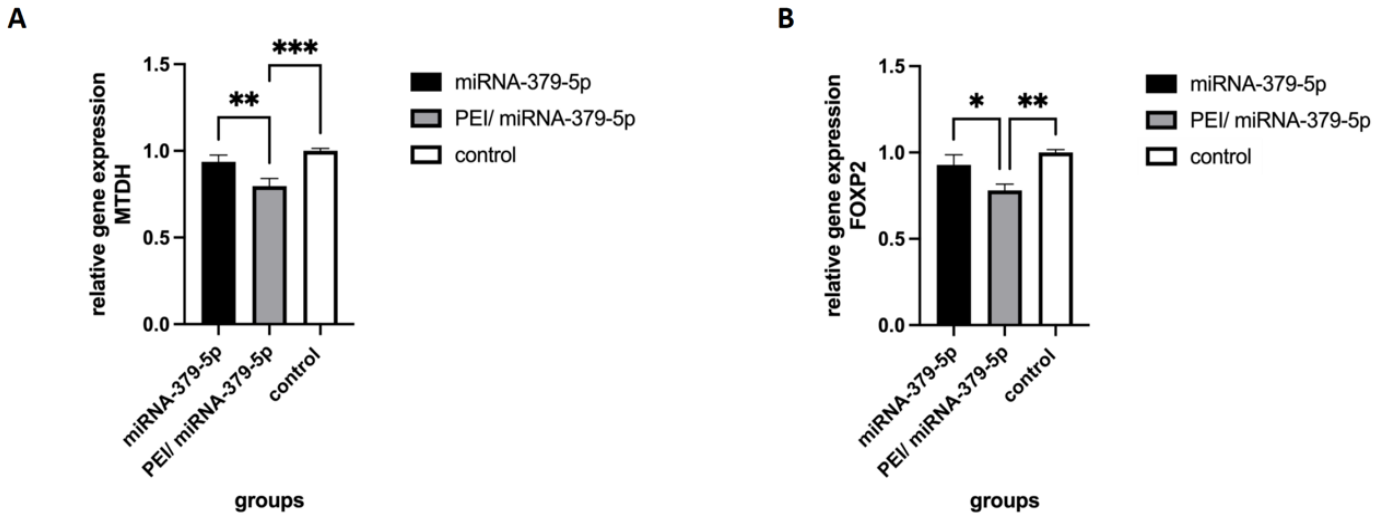

Figure 4. Relative mRNA expression levels of target genes MTDH (A) and FOXP2 (B) in Caco-2 cells. Cells were treated with naked miR-379-5p or PEI/miR-379-5p nanocomplexes (N:P 20:1, 50 nM) for 48 h. Gene expression was quantified using RT-qPCR and normalized to the internal reference gene ACTB (β-actin). Data are presented as fold change relative to the control group (set to 1.0). Values represent the mean ± SD of three independent experiments (n = 3). Statistical significance was determined using one-way ANOVA with Tukey's post-hoc test; significance levels were indicated as *p < 0.05, **p < 0.01, and ***p < 0.001 compared to the untreated control group.

SD: Standard deviation, ACTB: β-actin, MTDH: Metadherin, FOXP2: Forkhead box P2, ANOVA: Analysis of variance, RT-qPCR: Reverse transcription quantitative polymerase chain reaction, PEI: Polyethylenimine..

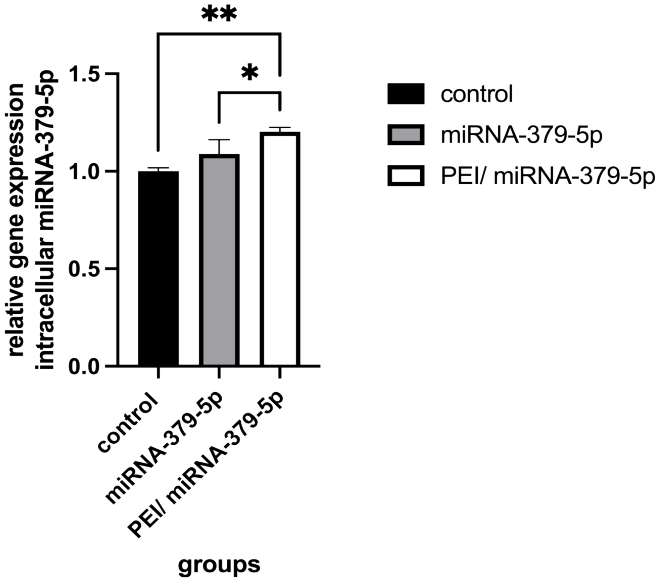

Figure 5. Intracellular accumulation of miR-379-5p in Caco-2 cells. The relative intracellular expression of miR-379-5p was determined by RT-qPCR following 48 h of incubation with either naked miRNA or PEI-miRNA nanocomplexes (N:P 20:1) at a final miRNA concentration of 50 nM. Data are presented as fold changes relative to the control group (set to 1.0) after normalization to the internal reference gene. Values represent the mean ± SD of three independent experiments (n = 3). Statistical significance was analyzed using one-way ANOVA with Tukey's post-hoc test: *p < 0.05 versus naked miRNA; **p < 0.01 versus untreated control.

SD: Standard deviation, ANOVA: Analysis of variance, RT-qPCR: Reverse transcription quantitative polymerase chain reaction, PEI: Polyethylenimine.

DISCUSSION

The development of efficient and safe delivery systems remains the primary bottleneck in the clinical translation of RNAi therapeutics. In this study, we engineered and optimized a PEI-based nanocarrier system for the intracellular delivery of miR-379-5p into CRC cells. Our findings demonstrate that the optimized PEI-miRNA nanocomplexes (N:P ratio 20:1) possess physicochemical characteristics favorable for cellular uptake, exhibit a manageable toxicity profile at therapeutic concentrations, and significantly enhance silencing of the oncogenic targets MTDH and FOXP2 compared with naked miRNA.

The physicochemical properties of nanoparticle systems, specifically hydrodynamic diameter and surface charge, are critical determinants of their biological fate and cellular internalization efficiency (36). Our DLS data revealed that increasing the N:P ratio resulted in more compact nanoparticles, with the 20:1 formulation yielding a mean diameter of approximately 254 nm. While particles in the 200 nm range are classically described as entering cells via clathrin-mediated endocytosis, recent evidence suggests that strict monodispersity may not be the sole prerequisite for effective delivery. González-Domínguez et al. (37) recently demonstrated that micrometric DNA/PEI aggregates (450-650 nm) can actually correlate with higher transient gene expression yields compared to smaller counterparts. This enhanced efficacy is attributed to the uptake of larger complexes via macropinocytosis and their subsequent accumulation near the nuclear envelope, where they function as a sustained "reservoir", progressively releasing the genetic cargo. Consequently, the slight polydispersity observed in our system may functionally contribute to the therapeutic effect by enabling exploitation of multiple entry pathways, including clathrin-mediated uptake of smaller fractions and macropinocytosis of larger aggregates. Furthermore,

morphological analysis via SEM confirmed that the nanocomplexes possess a compact, spherical structure. The particle size observed in SEM micrographs (~180-220 nm) was slightly smaller than the hydrodynamic diameter measured by DLS (~254 nm). This difference is anticipated and characteristic of polymeric systems, as DLS measures the hydrodynamic radius, including the hydration shell, in the aqueous phase, whereas SEM depicts the particles in a dehydrated solid state.

Concomitant with the size reduction, we observed a substantial increase in zeta potential, reaching +56.9 mV at the optimized ratio. This high cationic charge serves a dual purpose: first, it ensures the colloidal stability of the dispersion through electrostatic repulsion, thereby reducing particle aggregation in suspension (38). This high zeta potential was measured in nuclease-free water, reflecting the inherent colloidal stability of the formulation; however, under physiological conditions, the effective surface charge is expected to decrease due to ionic screening and protein corona formation. Secondly, and perhaps more critically, it facilitates the initial electrostatic adsorption of the nanocomplexes onto the negatively charged proteoglycans of the cell membrane, a prerequisite for efficient endocytosis (39). The agarose gel retardation assays corroborated these findings by showing that a 20:1 ratio provided sufficient cationic density to fully neutralize and condense miRNA, thereby protecting it from premature degradation—a crucial feature given the inherent instability of naked RNA in physiological environments.

While the high cationic charge density of PEI is advantageous for cellular uptake and promotes the “proton sponge” effect, which facilitates endosomal escape, it is also the primary source of PEI-mediated cytotoxicity. Our viability assays in Caco-2 cells revealed a concentration-dependent toxicity profile. While the formulation was well tolerated at 10 nM and 50 nM, viability dropped significantly at 100 nM. This observation is consistent with literature attributing PEI toxicity to membrane disruption and mitochondrial damage caused by an excess of free polycations (40). Consequently, the identification of 50 nM as the optimal working concentration represents a critical balance between maximizing therapeutic payload and preserving cellular health.

To explicitly validate the transmembrane transport of the therapeutic cargo, we analyzed intracellular miRNA levels (Figure 4), providing direct evidence of the nanocarrier’s transport efficiency. While cells treated with naked miR-379-5p showed negligible intracellular accumulation, likely due to electrostatic repulsion between the negatively charged RNA and the cell membrane, the PEI-complexed group exhibited a statistically significant increase in intracellular miRNA abundance ($p<0.01$). This confirms that the optimized nanocomplexes effectively shielded the miRNA’s charge and utilized the cationic PEI surface to facilitate transmembrane crossing, likely via endocytic pathways.

Building on this efficient internalization, we validated the functional capability of the delivered cargo by assessing downstream gene targets. We utilized miR-379-5p, a tumor suppressor often downregulated in various malignancies, to validate our system. The significant downregulation of MTDH and FOXP2 observed in the PEI-complexed group confirms successful gene silencing. Although the formulation was optimized to minimize acute cytotoxicity at this concentration, the robust suppression of these oncogenes suggests significant therapeutic potential through restoration of the miR-379-5p regulatory axis. Although the reduction in mRNA levels appears modest (~16-20%), miRNAs primarily function through translational repression. Therefore, the protein-level suppression might be more profound than what is observed at the transcript level, warranting future proteomic validation. Our observation that FOXP2 silencing promotes cell death stands in contrast to previous reports, such as Liao et al. (33), which characterized FOXP2 as a tumor suppressor that inhibits pyroptosis in CRC. However, this discrepancy can be attributed to the specific genetic context of the cell lines used. A recent study by Liu et al. (31) demonstrated that the function of FOXP2 in colorectal cancer is dictated by KRAS mutation status. While FOXP2 acts as a suppressor in KRAS-mutant cells, its high expression is associated with poor prognosis and adverse clinical outcomes in KRAS-wild-type patients. Since Caco-2 cells are KRAS-wild-type, the high expression of FOXP2 likely supports tumor progression in this model. Therefore, our findings support the therapeutic utility of targeting FOXP2 in KRAS-wild-type CRC subtypes and further emphasize the need for personalized RNAi strategies based on genetic biomarkers.

Study Limitations

Despite the promising results, certain limitations warrant mention. First, the biological evaluation was conducted *in vitro* using a Caco-2 model, which cannot fully replicate systemic physiological barriers or protein-corona effects, necessitating future *in vivo* validation. Second, while transcriptional silencing was confirmed via RT-qPCR, protein-level validation has yet to be performed to fully quantify functional suppression. Given that the therapeutic benefit of targeting FOXP2 is linked to the KRAS-wild-type genotype, the applicability of this strategy to KRAS-mutant subtypes of colorectal cancer requires further comparative investigation.

CONCLUSION

In this study, we engineered a cationic polymer-based nanocarrier system for effective delivery of the tumor suppressor miR-379-5p to colorectal cancer cells. Through systematic physicochemical optimization, the 20:1 PEI-miRNA formulation was identified as the ideal candidate, exhibiting a high cationic charge (+56.9 mV) that promotes stability and cellular uptake, while maintaining a manageable toxicity profile at therapeutic concentrations (50 nM). Although the particles displayed some polydispersity, this heterogeneity likely facilitates multiple cellular entry pathways, including macropinocytosis, thereby enhancing the functional delivery of the genetic cargo. Biological evaluation confirmed that these nanocomplexes significantly downregulated the oncogenic targets MTDH and FOXP2, restoring the tumor-suppressive molecular profile of miR-379-5p, thereby establishing a foundation for inhibiting tumor progression. Collectively, these findings validate the 20:1 PEI-miRNA system as a promising platform for RNAi-based precision oncology and warrant further investigation in colorectal cancer models *in vivo*.

Ethics

Ethics Committee Approval: Ethical approval was not required for this study, as no human participants or animal subjects were involved.

Informed Consent: Informed consent was not required because the study did not require ethics committee approval.

Footnotes

Authorship Contributions

Surgical and Medical Practices: E.Ç., E.K., C.B., Ç.A., M.B.K., S.A.A., Y.E.K., Concept: E.Ç., E.K., C.B., Ç.A., M.B.K., S.A.A., Y.E.K., Design: E.Ç., E.K., C.B., Ç.A., M.B.K., S.A.A., Y.E.K., Data Collection or Processing: E.Ç., E.K., C.B., Ç.A., M.B.K., S.A.A., Y.E.K., Analysis or Interpretation: E.Ç., E.K., C.B., Literature Search: E.Ç., E.K., C.B., Writing: E.Ç., E.K., C.B., Ç.A., M.B.K., S.A.A., Y.E.K.

Conflict of Interest: No conflict of interest was declared by the authors.

Financial Disclosure: This study was supported by the Scientific and Technological Research Council of Türkiye (TÜBİTAK-BIDEB) under Project No. 1919B012433754.

Acknowledgment

The authors would like to thank all colleagues who provided valuable input during the development of this study. In particular, we are grateful to Beyza Şahin, Nisa Nur Topaloğlu, Ebrar Dilanur Özben, and Yasemin Nişancı for their assistance and support.

REFERENCES

1. Siegel RL, Jakubowski CD, Fedewa SA, Davis A, Azad NS. Colorectal cancer in the young: epidemiology, prevention, management. Am Soc Clin Oncol Educ Book. 2020; 40: 1-14.
2. Tsai KY, Huang PS, Chu PY, Nguyen TNA, Hung HY, Hsieh CH, et al. Current applications and future directions of circulating tumor cells in colorectal cancer recurrence. Cancers (Basel). 2024; 16: 2316.
3. Goel A, Rastogi A, Jain M, Niveriya K. RNA-based therapeutics: past, present and future prospects, challenges in cancer treatment. Curr Pharm Biotechnol. 2024; 25: 2125-37.
4. Pallathadka H, Hsu CY, Obaid Saleh R, Renuka Jyothi S, Kumar A, Yumashev A, et al. Specific small interfering RNAs (siRNAs) for targeting the metastasis, immune responses, and drug resistance of colorectal cancer cells (CRC). Int Immunopharmacol. 2024; 140: 112730.
5. Xu R, Du A, Deng X, Du W, Zhang K, Li J, et al. tsRNA-GlyGCC promotes colorectal cancer progression and 5-FU resistance by regulating SPIB. J Exp Clin Cancer Res. 2024; 43: 230.
6. Al-Jumaili MMO. A potential interpretation of RNA interference and GC island modification in progressive colorectal cancer suppression. Biomed Biotechnol Res J. 2023; 7: 425-31. Available from: https://journals.lww.com/bbrj/fulltext/2023/07030/a_potential_interpretation_of_rna_interference_and.16.aspx.
7. Castellano M, Blanco V, Calzi ML, Costa B, Witwer K, Hill M, et al. Ribonuclease activity undermines immune sensing of naked extracellular RNA. bioRxiv [Preprint]. 2024: 2024.04.23.590771.
8. Muskan M, Abeysinghe P, Cecchin R, Branscome H, Morris KV, Kashanchi F. Therapeutic potential of RNA-enriched extracellular vesicles: The next generation in RNA delivery via biogenic nanoparticles. Mol Ther. 2024; 32: 2939-49.
9. Zhang H, Vandesompele J, Braeckmans K, De Smedt SC, Remaut K. Nucleic acid degradation as barrier to gene delivery: a guide to understand and overcome nuclease activity. Chem Soc Rev. 2024; 53: 317-60.
10. Wei PS, Thota N, John G, Chang E, Lee S, Wang Y, et al. Enhancing RNA-lipid nanoparticle delivery: Organ- and cell-specificity and barcoding strategies. J Control Release. 2024; 375: 366-88.
11. Domingues C, Jarak I, Coelho J, Carvalho RA, Veiga F, Vitorino C, et al. Optimizing pluronic-PEI nanocarriers for RNAI delivery in oral cancer: from polymer synthesis to functional screening. Biomacromolecules. 2025; 26: 7484-511.
12. Gonzalez-Melero L, Santos-Vizcaino E, Varela-Calvino R, Gomez-Tourino I, Asumendi A, Boyano MD, et al. PLGA-PEI nanoparticle covered with poly(I:C) for personalised cancer immunotherapy. Drug Deliv Transl Res. 2024; 14: 2788-803.
13. Li R, Yu K, Fan G-C, Song Z, Luo X. Polyethyleneimine cross-linked BSA with enhanced antifouling capability for electrochemical detection of cancer antigen 125 in complex biofluids. Sens Actuators B Chem. 2024; 408: 135520.
14. Yang S, Wu Y, Zhong W, Chen R, Wang M, Chen M. GSH/pH dual activatable cross-linked and fluorinated pei for cancer gene therapy through endogenous iron de-hijacking and *in situ* ROS amplification. Adv Mater. 2024; 36: e2304098.
15. Huang P, Deng H, Zhou Y, Chen X. The roles of polymers in mRNA delivery. Matter. 2022; 5: 1670-99.
16. Berger S, Lächelt U, Wagner E. Dynamic carriers for therapeutic RNA delivery. Proc Natl Acad Sci U S A. 2024; 121: e2307799120.
17. Lübbersmeyer TL, Wissel K, Hoffmann A, Kötter L, Lenarz T, Paasche G. Establishing a non-viral transfection system for fibroblasts using branched polyethylenimine. PLoS One. 2025; 20: e0329666.
18. Ismail A, Chou SF. Polyethylenimine Carriers for Drug and Gene Delivery. Polymers (Basel). 2025; 17: 2150.
19. Samadi P, Rahbarizadeh F, Nouri F, Soleimani M, Najafi R, Jalali A. MUC1-driven guanylin gene delivery via succinylated PEI-9 nanocarrier for colorectal cancer treatment: an *in silico* and *in vitro* study. Adv Pharm Bull. 2025; 15: 844-70. Available from: https://apb.tbzmed.ac.ir/Article/apb-45741
20. Lee GY, Lo PY, Cho EC, Zheng JH, Li M, Huang JH, et al. Integration of PEG and PEI with graphene quantum dots to fabricate pH-responsive nanostars for colon cancer suppression *in vitro* and *in vivo*. FlatChem. 2022; 31: 100320.
21. Jiazhen N, Meihui S, De-E L, Na L, Youtao X, Qixian C, et al. Remodeling the inflammatory and immunosuppressive tumor microenvironment for enhancing antiangiogenic gene therapy of colorectal cancer. Adv Healthc Mater. 2025; 14: e2402887.
22. Lin G, Huang J, Zhang M, Chen S, Zhang M. Chitosan-crosslinked low molecular weight pei-conjugated iron oxide nanoparticle for safe and effective DNA delivery to breast cancer cells. Nanomaterials (Basel). 2022; 12: 584.
23. Peng Y, Gao Y, Yang C, Guo R, Shi X, Cao X. Low-molecular-weight poly(ethylenimine) nanogels loaded with ultrasmall iron oxide nanoparticles for T1-weighted MR imaging-guided gene therapy of sarcoma. ACS Appl Mater Interfaces. 2021; 13: 27806-13.
24. Wang C, Pan C, Yong H, Wang F, Bo T, Zhao Y, et al. Emerging non-viral vectors for gene delivery. J Nanobiotechnology. 2023; 21: 272.
25. Cassidy JR, Persson M, Voss G, Underbjerg KR, Ivkovic TC, Bjartell A, Edsjö A, Lilja H, Ceder Y. MicroRNA-379 modulates prostate-specific antigen expression through targeting the androgen receptor in prostate cancer. Cancers (Basel). 2025; 17: 3245.
26. Mosaad H, Abdelrahman AE, Abdullatif A, Lashin ME, Ramadan MSH, El-Azony A, et al. MIR-379-5p Expression in Endometrial

Cancer and Its Correlation with ROR1 Expression. Asian Pac J Cancer Prev. 2023; 24: 239-48.

27. Hu W, Cao W, Liu J. RETRACTED: LncRNA-NEAT1 facilitates autophagy to boost pemetrexed resistance in lung adenocarcinoma via the mir-379-3p/HIF1A pathway. Human & Experimental Toxicology. 2025; 43.
28. Srinath S, Jishnu PV, Varghese VK, Shukla V, Adiga D, Mallya S, et al. Regulation and tumor-suppressive function of the miR-379/miR-656 (C14MC) cluster in cervical cancer. Mol Oncol. 2024; 18: 1608-30.
29. Yang K, Li D, Jia W, Song Y, Sun N, Wang J, et al. MiR-379-5p inhibits the proliferation, migration, and invasion of breast cancer by targeting KIF4A. Thorac Cancer. 2022; 13: 1916-24.
30. Shukla D, Mishra S, Mandal T, Charan M, Verma AK, Khan MMA, et al. MicroRNA-379-5p attenuates cancer stem cells and reduces cisplatin resistance in ovarian cancer by regulating RAD18/Polη axis. Cell Death Dis. 2025; 16: 140.
31. Liu J, Wang Y, Liu Y, Mei H, Zhang Q, Gao Z, et al. FOXP2/SOS1/AKT negative feedback loop inhibits cell proliferation in KRAS-mutant colorectal cancer. Apoptosis. 2025; 30: 2455-65.
32. Huang R, Xiang G, Duan X, Wang H, He K, Xiao J. MiR-132-3p inhibits proliferation, invasion and migration of colorectal cancer cells via down-regulating FOXP2 expression. Acta Biochim Pol. 2022; 69: 371-7.
33. Liao P, Huang WH, Cao L, Wang T, Chen LM. Low expression of FOXP2 predicts poor survival and targets caspase-1 to inhibit cell pyroptosis in colorectal cancer. J Cancer. 2022; 13: 1181-92.
34. Çelik E, Bayram C, Denkbaş EB. Chondrogenesis of human mesenchymal stem cells by microRNA loaded triple polysaccharide nanoparticle system. Mater Sci Eng C Mater Biol Appl. 2019; 102: 756-63.
35. He Q, Zhao L, Liu Y, Liu X, Zheng J, Yu H, et al. circ-SHKBP1 regulates the angiogenesis of u87 glioma-exposed endothelial cells through miR-544a/FOXP1 and miR-379/FOXP2 pathways. Mol Ther Nucleic Acids. 2018; 10: 331-48.
36. Prabha S, Arya G, Chandra R, Ahmed B, Nimesh S. Effect of size on biological properties of nanoparticles employed in gene delivery. Artif Cells Nanomed Biotechnol. 2016; 44: 83-91.
37. González-Domínguez I, Puente-Massaguer E, Lavado-García J, Cervera L, Gòdia F. Micrometric DNA/PEI polyplexes correlate with higher transient gene expression yields in HEK 293 cells. N Biotechnol. 2022; 68: 87-96.
38. Wang Y, Ye M, Xie R, Gong S. Enhancing the *in vitro* and *in vivo* stabilities of polymeric nucleic acid delivery nanosystems. Bioconjug Chem. 2019; 30: 325-37.
39. Fröhlich E. The role of surface charge in cellular uptake and cytotoxicity of medical nanoparticles. Int J Nanomedicine. 2012; 7: 5577-91.
40. Grandinetti G, Ingle NP, Reineke TM. Interaction of poly(ethylenimine)-DNA polyplexes with mitochondria: implications for a mechanism of cytotoxicity. Mol Pharm. 2011; 8: 1709-19.